

## Amazonite in Pakistan: A Comprehensive Study with XRD, XPS, SEM and PL Analyses

Eren Cihan Karsu Asal <sup>1,a,\*</sup>

<sup>1</sup> Department of Electric and Energy Technologies, Manisa Celal Bayar University, 45400 Turgutlu Manisa, Türkiye.

\*Corresponding author

### Research Article

#### History

Received: 25/01/2023

Accepted: 04/04/2023

#### Copyright




©2023 Faculty of Science,  
Sivas Cumhuriyet University


### ABSTRACT

Although amazonite minerals from various locations have been studied before rather less attention has been paid to the amazonite mineral from Pakistan. The present work is presented an extensive structural characterization of natural amazonite aliquots (KAlSi<sub>3</sub>O<sub>8</sub>) from Tangir Valley, Gilgit-Pakistan. The phase and elemental analysis have been characterized by both X-ray Diffraction (XRD) and X-ray Photoelectron Spectroscopy (XPS), respectively. The surface morphology and particle size have been identified by Scanning Electron Microscopy (SEM). The luminescence properties have been investigated using PhotoLuminescence (PL). In addition, the lifetime of the PL emission measurements has been estimated.

Eventually, this microcline has a triclinic phase, mainly composed of (AlO<sub>4</sub>)<sup>-5</sup> ions, SiO<sub>2</sub>, metal SiO<sub>4</sub>, Al<sub>2</sub>O<sub>3</sub> and oxygen originating from impurities. The average particle size is around 1–10 µm with a complex structure. The PL spectrum has broad emission and excitation bands (520 nm and 340 nm respectively). The average lifetime of the PL emission is 265,21 µs. For the accuracy of the results all experiments were performed with not only a single aliquot, but with three aliquots, and representative results are presented.

**Keywords:** Photoluminescence, Amazonite, Characterization.

 [eren.karsu@cbu.edu.tr](mailto:eren.karsu@cbu.edu.tr)

 <https://orcid.org/0000-0001-6392-2668>

## Introduction

The importance of the crystalline phase, in both the analysis of various emission characteristics and lattice parameters is a well-known subject. Furthermore, any aspect of the luminescence phenomena, (e.g., lifetime, effectiveness, emission spectra) is known to be dependent on the crystalline phase which is primarily brought about by pressure and/or temperature. Minor changes in the lattice structure caused by inclusions, impurities, substituted ions, or surface defects in ppm concentrations display changes in the intensity and wavelength location of the emission spectra [1].

Recently there has been a growing interest in microcline, a variety of potassium-rich alkali feldspar. One of these, Amazonite, has blue green color because of its structure of one aluminum and three silicon ions (KAlSi<sub>3</sub>O<sub>8</sub>). The silicon and aluminum ions occupy the centers of interlinked tetrahedrons of SiO<sub>4</sub> and AlO<sub>4</sub> compounds. These tetrahedrons are connected at each corner to other tetrahedrons forming an intricate three-dimensional negatively charged framework [2]. While the simple form of this microcline has been reported as a monoclinic crystal, the triclinic form of this mineral is also observed [3].

Given the lack of attention paid to the amazonite mineral from Tangir Valley, Gilgit-Pakistan, the current study intends to achieve the following primary contributions, which are summarized as follows:

- This, in my opinion, is the first time an amazonite mineral from the Tangir Valley in Gilgit, Pakistan, has been thoroughly examined.
- This will be a thorough evaluation that includes all phase-elemental studies, surface morphology, particle size, and luminescence properties.
- The decay character of PL emission was measured, and the emission and excitation spectrums were studied.
- Each experiment used not only one aliquot but three aliquots to ensure the accuracy of the data.

## Materials and Methods

### 1. Sample Details and Preparation

The materials employed in the current study were natural aliquots of Amazonite crystal that were from Tangir Valley, Gilgit-Pakistan. Three aliquots of a single crystal that had been crushed in an agate mortar to a weight of 5.0±0.1 mg were utilized in each research, and representative findings were presented.

### 2. Apparatus and Measurement Conditions

i.Characterization:

An overlook of characterization was performed. In addition to both phase and elemental analysis by X-Ray Diffraction (XRD) and X-Ray Photoelectron Spectroscopy (XPS) technique, Scanning Electron Microscopy (SEM) patterns were also obtained to observe the particle morphology of the aliquots.

- XRD Technique:

The crystal structures and phase analysis of the natural amazonite were carried out at room temperature (RT) by using the Panalytical Emperian X-ray diffractometer with a Cu-K $\alpha$  radiation source ( $\lambda=1,5406 \text{ \AA}$ ). The system was operated at 45 kV voltage and 40 mA current.

For the qualitative test, XRD patterns were recorded at a speed of  $2,00^\circ/\text{min}$  in the interval of  $10^\circ\text{--}80^\circ$  ( $2\theta$ ). The step size was  $0,02^\circ$  and the interaction time was 0,6 seconds. The detector type was fixed slits. The scanning mode was continuous. Formation parameters were obtained from Rietveld refinement through the 2.71 version of the Maud program. The outcomes were tested with those of the ICSD 98-001-6597 df card (Figure 1. and Table 1). [4]

- XPS Technique:

The excellent spatial resolution of XPS examinations allowed the sensitive detection of the contents of the amazonite mineral and prevented contaminations that might be caused by tiny inclusions. As a result, the XPS analyses' conclusions have turned out to be far more reliable than those of the other techniques. For these reasons, the XPS technique was used to characterize the data about the materials' elements and chemical states.

In the system, called Thermo-Scientific, a monochromatic Al-K $\alpha$  (1486.7 eV) X-ray source and a beam size of 400 nm diameter were used. The calibration was performed concerning gold; 4f7/2. While spectral data acquisition, the pressure was held under  $5 \times 10^{-10}$  mbar. The scanning was performed in the range between  $-10$  and  $1350 \text{ eV}$ . For high-resolution elemental scanning, the pass energy was 30 eV. 20 scans from a single point were recorded. By using the curve fitting method via Thermo Avantage V5.65 programs both the binding energies and the deconvolution of the spectra were achieved (Figure 2 and Table 2) [4].

- SEM Patterns:

The surface morphology was estimated by SEM patterns (Figure 3). Utilizing an electron microscope (COXEM EM-30+) and high potential (30 kV) accelerating, the microstructures of the particles were evaluated. Similar to the study of Gliozzo et al., the samples were carbon coated and mounted directly on sample holders. No surface polishing was performed [5].

- ii. Optical Properties:

PL technique was used to investigate the optical properties. The PL studies were utilized at Time-Correlated Single Photon Counting (TCSPC). The decay period was also measured during PL experiments in addition to the emission and excitation spectra. A 15W xenon lamp was used. During tests, to obtain the Instrument Response Function (IRF), a non-fluorescing mixture of silica aerogel (LU-DOX 30%, Sigma Aldrich) in water was used. Before decaying, 24 hrs the mineral was held inside the device in the darkness. The decay character was then immediately set. Excitation with the xenon lamp was performed for 1 minute during the readout, and the parameters were obtained using repeated convolution and a weighted, nonlinear least squares method. The reduced chi-square test was applied to correctly fit the calculated and measured decay curves [4].

## Results

### 1. Phase analyses:

The phase purity and crystallinity of amazonite were examined by the XRD technique. The XRD pattern of the natural amazonite is shown in Figure 1 The reference XRD pattern is also stated for comparison in the figure.

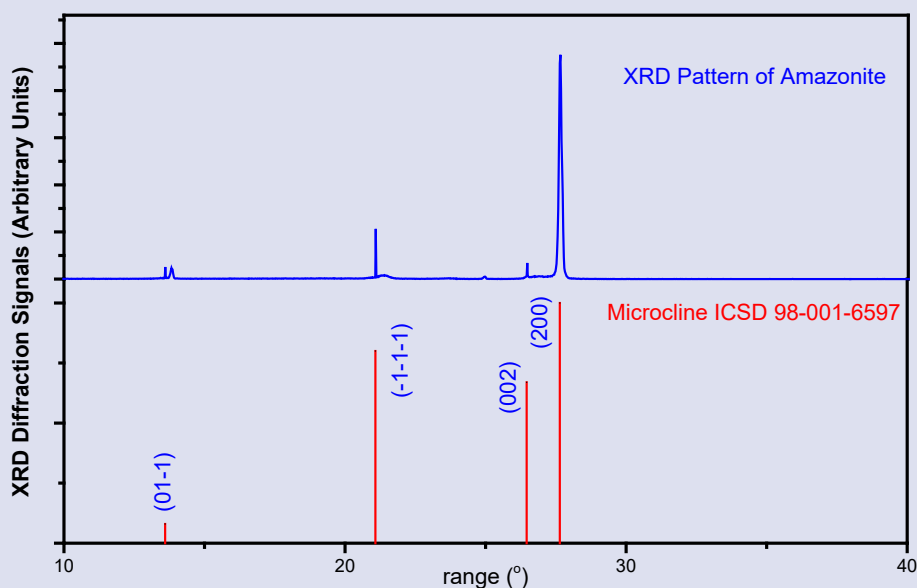


Figure 1. The basal latencies of rats before and after operation (paired student t-test, \* $p < 0.05$ )

By comparing the XRD peaks with The Joint Committee on Powder Diffraction Standards (JCPDS) file, the peaks were indexed by International Centre for Diffraction Data (ICSD) and matches precisely with standard data ICSD 98-001-6597. The diffraction peaks of the amazonite are well indexed to a triclinic phase structure of amazonite (Figure 1) [6]. Structural and lattice parameters of amazonite

were calculated with the Rietveld refinement using the Maud 2.71 V software. The results obtained from the patterns are indicated in Table 1 Here, it was discovered that the structural parameters a and c were quite tight to one another (8,59 and 7,22 Å respectively).

**Table 1.** The results of XRD patterns of the amazonite sample:

Mineral		Crystal System	Unit Cell Parameters					
Name	Formula		a(Å)	b(Å)	c(Å)	$\alpha(^{\circ})$	$\beta(^{\circ})$	$\gamma(^{\circ})$
Microcline (amazonite)	KAlSi <sub>3</sub> O <sub>8</sub>	Triclinic	8,59	12,97	7,22	90,6	116	87,8

## 2. Elemental analysis:

The valence states, chemical nature and oxidation of numerous elements in the natural amazonite aliquots were characterized using XPS, as marked in Figure 2. It is a representation of the findings from the analysis and high-resolution elemental detects of the aliquot. Table 2 presents specifically the binding energies of the present elements and the weight ratios of the analyses. The observed C1s is taken as an impurity of the system. The peaks at 284 and 286 eV belong to C-C and C-O bonding respectively. These peaks were observed because of the hydrocarbon at the medium where the XPS measurements were performed. Moreover, Na1s was peeked, but with a trace amount, only 0,88%. Figure 2(a)

remarks on the regular scanning of the aliquot. 531.03 eV for O1s, 102.89 eV for Si2p, 293.53 eV for K2p, and 74.71 eV for Al2p are revealed for the mineral. Figure 2(b)-(e) represents just the detailly scanning of each large amount element. Figure 2(b) shows the peaks of Al-O bonds (~74-75 eV) originating from (AlO<sub>4</sub>)<sup>-5</sup> ions. In Figure 2(c), Si2p oxidation state is represented by two peaks, these originating from SiO<sub>2</sub> and metal SiO<sub>4</sub> (102,5-1.3,5 eV). K2p deconvolution with three elemental peaks (~292,5-293,5-296 eV) is given in Figure 2(d), and Figure 2(e) marks the high-resolution deconvoluted peak of O1s. Three peaks were observed at around 529,5-531-532 eV which are belongs to SiO<sub>2</sub>, Al<sub>2</sub>O<sub>3</sub>, and organic oxygen originating from impurities.

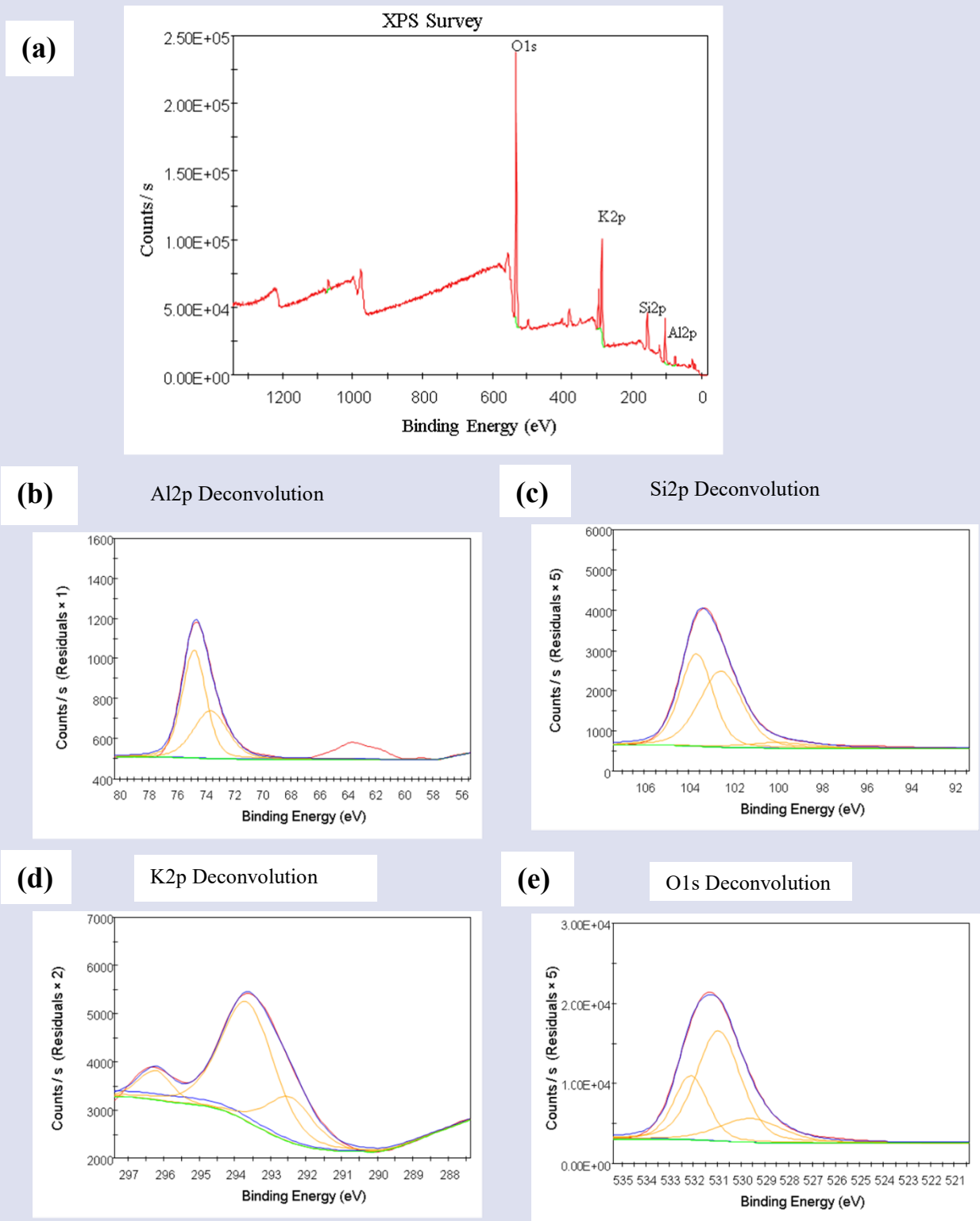


Figure 2 XPS (also known as ESCA) spectrum of amazonite. (a) survey and deconvoluted (b) Al2p, (c) Si2p, (d) K2p, (e) O1s

**Table 2** XPS outcomes of natural amazonite aliquots

Sample	Elements	Binding Energy (eV)			Survey weight (%)	
		Survey B.E.	Decay Elemental B.E.			
			1st peak	2nd peak		3rd peak
Amazonite	O 1s	531.03	529,5	531	532	35.82
KAlSi <sub>3</sub> O <sub>8</sub>	C 1s	284.41	284	285	-	25.43
	Si 2p	102.89	102,5	103,5	-	24.49
	K 2p	293.53	292,5	293,5	296	6.80
	Al 2p	74.71	74	75	-	6.59
	Na 1s	1068.75	1071	1072	-	0.88

### Surface Morphology & Particle Size:

Regarding the imaging purpose and morphology of the mineral, there are smooth micro monolithic surfaces with tiny hollows (pore diameter is  $\sim 0,2-1 \mu\text{m}$ ) on the surface and small pieces ( $\sim 0,2-3,5 \mu\text{m}$ ) all around. The average particle size of amazonite was found to be  $1-10 \mu\text{m}$  (Figure 3). The given  $\alpha$  and  $\gamma$  crystallographic angles are very close to  $90^\circ$  (Table 1).

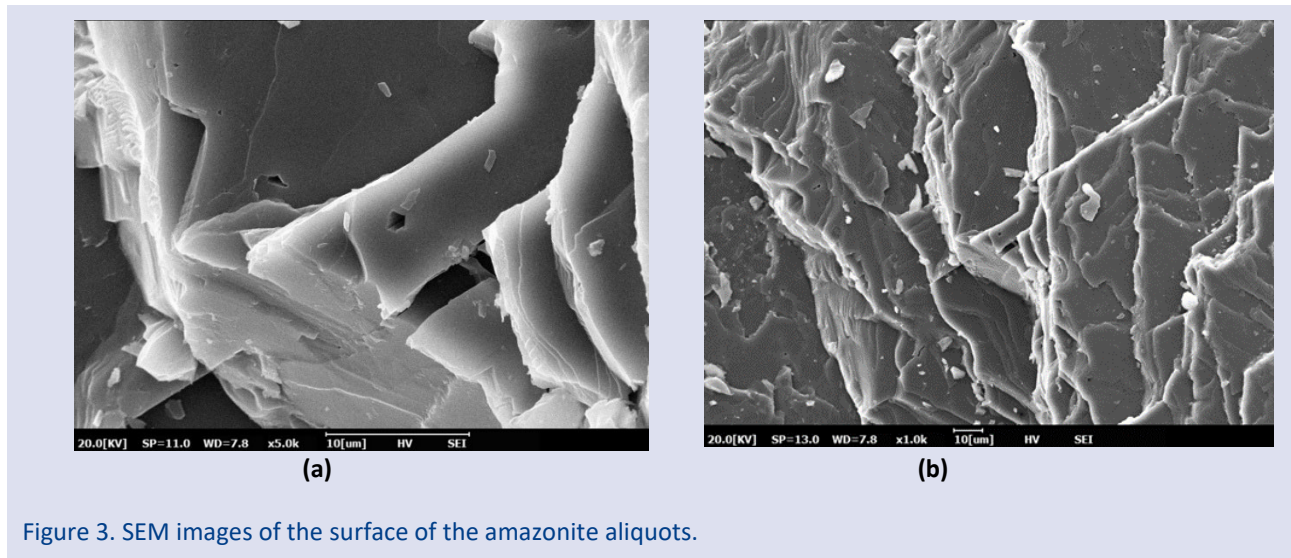


Figure 3. SEM images of the surface of the amazonite aliquots.

### Optical Analysis

Figure 4 represents not only the excitation and emission bands but also the PL decay curves of amazonite aliquots. Figure 4(a) states the excitation and emission spectrum at RT of the mineral. The excitation spectrum of emission has a wide band (250- 500 nm) making a peak around 340 nm, corresponding to the host lattice transition. The excitation range is noted in the UV-blue region of the electromagnetic spectrum. The emission peak under excitation launches from 360 nm and gives broadband that lasts at around 650 nm. The summit of the emission peak was detected at around 520 nm which is attributed to the blue-green colour of the amazonite. A long afterglow is observed (Figure 4(b))

The decaying duration of the amazonite mineral at RT was also tested (Table 3 and Figure 4(b)). The decay data was monitored afterward the excitation was ended and the decaying duration was calculated using the exponential formula's principle. [4]. In Figure 4(b) it is marked that, the decay curves and the long-lasting phosphorescence of the amazonite mineral consist of two main sections: the fast-decaying section and the slow-decaying section, which is given in detail with empirical equations by Gultekin et al. [4].

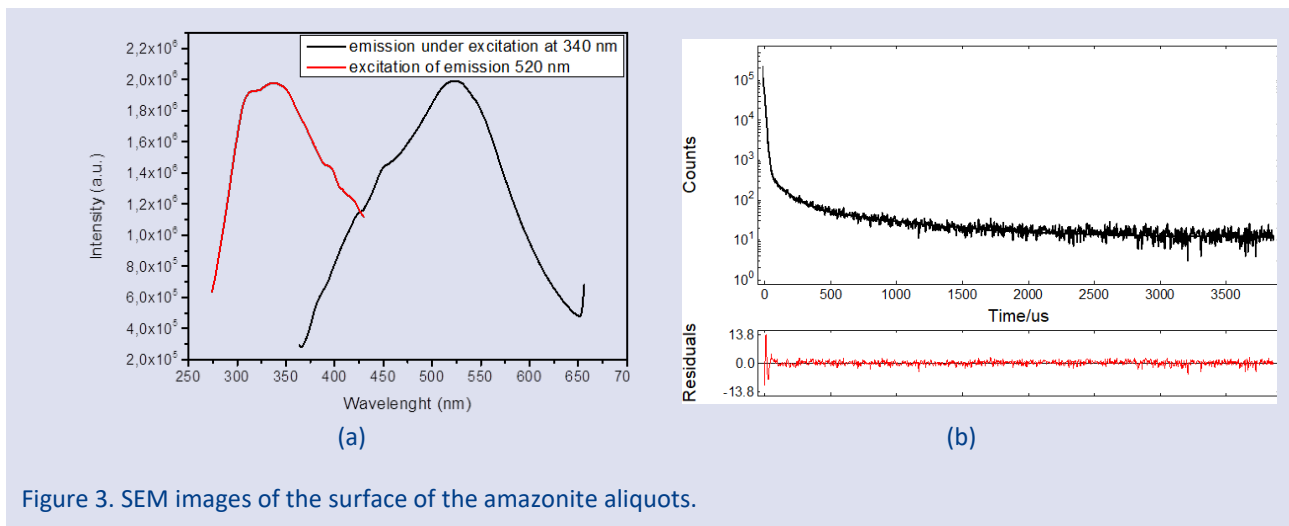


Figure 3. SEM images of the surface of the amazonite aliquots.

In Table 3.  $\tau_1$ ,  $\tau_2$  and  $\tau_3$  are the decaying durations. The amazonite aliquot showed three exponential decaying durations. The short lifetime (9.13  $\mu\text{s}$ ), the middle lifetime (103.76  $\mu\text{s}$ ), and the long lifetime (682,75  $\mu\text{s}$ ) components were noted.

**Table 3** Excitation and emission wavelength and decay time measurement results of amazonite aliquots with standard deviation and percentage distribution

Sample	Excitation wavelength (nm)	Emission wavelength (nm)	$\chi^2$		Decay Period ( $\mu\text{s}$ )	Standard Deviation	Rel.%
KAISi <sub>3</sub> O <sub>8</sub>	340	520	1.765	$\zeta_1$	9.13	318.4296	85.25
				$\zeta_2$	103.76	16.6616	7.09
				$\zeta_3$	682.75	4.1549	7.66
				$\zeta_{avr}$	265,21		

## Discussion

The initial step of the study included structural phase analysis, elemental analyses, structure morphology, and particle size since both the formation and crystallinity have a significant impact on the luminescence curves. It has long been understood that all the features of the luminescence phenomena, including lifetime, efficiency, and emission spectra, are dependent on the crystalline phase, which is primarily induced by temperature and pressure [1]. The second step was the PL characteristics.

Amazonite has been the subject of numerous studies regarding its luminescence properties, but it is well known that changes in the intensity and wavelength position at emission spectra can be caused by even minute variations in the lattice structure caused by inclusions, impurities, substituted ions, or surface defects in ppm concentrations [1]. For this reason, the amazonite mineral sample from Tangir Valley, Pakistan, was carefully examined. Below is a detailed explanation of the collected results.

### 1. Phase & Elemental Properties:

The diffraction pattern of the amazonite observed in this study is compatible with the results in the literature [6]. Furthermore, while most feldspars have monoclinic structures, the amazonite investigated possesses a triclinic structure. The formation of triclinic microcline is possible by the transformation of monoclinic K-feldspar upon cooling [7] or by K-replacement of Na/Ca feldspar

[6]. The study by Deer et al. explains this circumstance by providing a detailed explanation of the microcline framework [8]. As they indicated, the K(Al,Si)O<sub>4</sub> tetrahedra that make up the crystal lattice of K-feldspars, known as amazonite, are joined to four other tetrahedra at their edges by shared or bridging O-1, providing a continuous and interconnected structure [9]. The framework contains four tetrahedral locations. The two of each are referred to as T1 and T2 sites and are occupied by Si<sup>4+</sup> or Al<sup>3+</sup>. The structure also includes a net negative charge that is balanced by massive K<sup>+</sup> cations that are in gaps called M-sites [8, 9]. Al<sup>3+</sup> has an equal chance of occupying any of the four tetrahedral places at the framework of amazonite in high temperatures [8]. During gradual cooling, as the framework shrinks, Al<sup>3+</sup> diffuses to occupy one of the two T1-sites and monoclinic low sanidine develops [8]. With continuous slow cooling, Al<sup>3+</sup> diffuses into the other T1-site, causing a symmetry change from monoclinic to triclinic, which is the structure of the amazonite examined in this work [8, 9]. For more information, the authors refer to Deer et al. 's book [8].

As the weight % values of elements given by the XPS technique are defined in Table 2 Na1s with 0,88% noted. This small amount is an impurity at KAISi<sub>3</sub>O<sub>8</sub> which may cause emission. The potential of this emission has already been emphasized by many scientists. The other observing impurity is C1s with 25,43 %. Inside the XPS system, there



were hydrocarbon impurities, for this reason, 284 and 286 eV peaks, which are indicating C-C and C-O bindings were observed, respectively. As both C-C and C-O bonds are not related to  $\text{KAlSi}_3\text{O}_8$  and just because of the pollution of the system C1s deconvolution is not given in Figure 2

## 2. Surface Morphology & Particle Size:

While in the literature it has been reported that (a) K-feldspar contains macropores of 0.1-1  $\mu\text{m}$  diameter [10] and (b) it has been common to see symmetrical intergrowth with a triclinic microcline because of the triclinic structure in feldspars [10, 11]; In the current study (a) the average particle size of amazonite was found to be 1-10  $\mu\text{m}$  (Figure 3) and (b) the given  $\alpha$  and  $\gamma$  crystallographic angles are very close to  $90^\circ$  (see Table 1), therefore it is tough to detect symmetrical intergrowth structures in SEM patterns since the surface would need to be slightly tilted. Similar to the findings of Welti et al. [6], both the obtained SEM and XRD patterns in the current study are in good agreement with the patterns of amazonite from Namibia [6], where height above sea level and geographic conditions are similar. Furthermore, for K-feldspars Hodson emphasized that the contribution of pores to the total particle surface increases with decreasing particle sizes [6, 12].

Related to the obtained results, it can be remarked that amazonite aliquots display a complex structure due to the complexity of their geological origin. This result is in line with earlier research, which revealed that this mineral's structure has several planar defects, including twinning and exsolution interphases [1, 6]. These defects can hold both hydroxyl groups and water molecules. In addition to planar defects, point defects that behave as luminescence centres may also occur. Considering this circumstance, structural defects can be the cause of the detected blue-green emission (it can be concluded that structural defects are one of the causes of the detected blue-green emission). Furthermore, Correcher and Garcia-Guinea underlined that the structure defect associated with emission can occur at the twin-domain boundaries, where ionic alkali self-diffusion, irreversible water losses, and irreversible dihydroxylation processes occur [1].

## 3. Optical Properties:

The achieved PL emission under excitation of 340 nm is broadband (from 360 to 650 nm) with a peak at 520 nm. This emission determines the blue-green colour of the microcline aliquot. The literature has also reported the presence of this emission, particularly for samples of amazonite from the Transbaikal, Ploskaia Mountain (Slovenia), Kola Peninsula, Urals, Kazakhstan, and Transbaikal [1, 3]. I now have this emission peak for amazonite samples from Tangir Valley in Gilgit-Pakistan.

Riedesel et al. found that the emission at 520 nm is brighter than the other dimmer-disclosed emissions at 300, 400, and 700 nm [9] and stated that this emission is disclosed at about  $170^\circ\text{C}$  [9]. The results of this study involving the PL results are well consistent with their findings.

The examined amazonite is thought to be nonvolcanic [13] because it has been noted that volcanic feldspars fade more quickly than those formed by nonvolcanic processes [14]. Regarding the system of the long afterglow, the long lifetime components are attributed to afterglow properties [4]. The first decay process results from the short survival time of the electron while the slow decay process could be attributed to the deep trap energy centre of the host lattice. The "hole-trapped-transported-retrapped" process has already been known as the reason for the phosphor's long afterglow [4]. Besides, long-lasting PL can be attributed to hole mobility, e-hole recombination, and a low rate of hole mobility, all of which rise the possibility of re-trapping and slowing down the decaying process [15]. Moreover, the mineral's fluorophore property could be caused by (1) structural defects located in the twin-domain borders, which could include ionic alkali-self-diffusion, irreversible water losses, and irreversible de-hydroxylation processes, (2) the intricate structure of amazonite, which contains several points and planar impurities (Na, Table 2) that can function as luminescence centres, (3) any continuity in the distribution of traps [1]. Although Gomez-Gonzales et al. stressed that, the blue-green colour of amazonite is related to the amount of lead or rubidium contents, this is not always the case, as demonstrated by this study [16].

## Conclusion

Up to now, the partially investigated amazonite mineral from Talgir Valley Pakistan is studied in detail on both crystal morphology and luminescence properties. The present conclusions can be summarized as follows:

### 1. Surface Morphology, Particle Size, Phase and Elemental Properties:

It is observed that both the crystal's structural state and the kind of its interfaces play a great role in determining the mineral's luminescence qualities [9].

The analysed amazonite has a triclinic structure. A trace amount of Na, 0.88 wt%, was found by XPS studies in addition to the components O, C, Si, K, and Al. This impurity is a type of point defect that can act as a luminescence centre. However, the characteristic UV emission of Na was not observed in the current investigation, and this might be caused by the minute levels of Na. The emission might also be moved to the blue. Amazonite aliquots have a complex structure, as evidenced by SEM micrographs. The size of macropores ranges from 0.1 to 1  $\mu\text{m}$ .

### 2. Optical Properties:

Blue-green emission spectra ( $\lambda_{\text{max}} = 520\text{ nm}$ ) were observed when the material was stimulated with 340 nm UV light. For the current microcline, this emission is thought to be caused by defects originating from a hole in the middle of an Al-O1- bridge ( $\text{Al}^{3+}\text{-O1--Al}^{3+}$ ) [9, 17]. The study of Krbetschek et al. is a comprehensive review of emission centers associated with crystal defects in

feldspars, hence I offer this publication for further studies on emission centers of feldspars [18].

In the current study, the afterglow properties of amazonite have been reported, and three different decay times were observed. It has been thought that the longest decay duration is due to deep traps formed during host lattice transitions.

## Acknowledgment

The author would like to acknowledge Associated Professor Serdar Yıldırım for his valuable technical assistance.

## Conflicts of interest

There are no conflicts of interest in this work.

## References

- [1] Correcher V., and Garcia-Guinea J., Study of The Luminescence Properties of a Natural Amazonite, *Radiation Measurements*, 46 (2011) 971-974.
- [2] Mittani J., Cano N., and Watanabe S., Use of [Pb-Pb]<sup>3+</sup> Center of The Amazonite for Dating, *Applied Radiation and Isotopes*, 62 (2005) 251-254.
- [3] Ostrooumov M., *Amazonite: Mineralogy, Crystal Chemistry, and Typomorphism*, Amsterdam, Boston, Heidelberg, London, New York, Oxford, Paris, San Diego, San Francisco, Singapore, Sydney, Tokyo: Elsevier (2008).
- [4] Gultekin S., Yıldırım S., Yılmaz O., Keskin I., and Kati M., Structural and Optical Properties of SrAl<sub>2</sub>O<sub>4</sub>: Eu<sup>2+</sup>/Dy<sup>3+</sup> Phosphors Synthesized by Flame Spray Pyrolysis Technique, *Journal of Luminescence*, 206 (2019) 59-69.
- [5] Gliozzo E., Mattingly D., Cole F., and Artioli G., In the Footsteps of Pliny: Tracing the Sources of Garamantian Carnelian from Fazzan, South-West Libya, *Journal of Archaeological Science*, 52 (2014) 218-241.
- [6] Welti A., Lohmann U., and Kanji Z., Ice Nucleation Properties of K-Feldspar Polymorphs and Plagioclase Feldspars, *Atmospheric Chemistry and Physics Discussions*, 19 (16) (2019) 10901-10918.
- [7] Waldron K., and Parsons I., Solution-Redeposition and the Orthoclase Microcline Transformation: Evidence from Granulites and Relevance to 18O Exchange, *Mineralogical Magazine*, 57 (1993) 687-695.
- [8] Deer W., Howie R., and Zussman J., *An Introduction to the Rock-Forming Minerals*, 3rd edition, London: The Mineralogical Society, 2013.
- [9] Riedesel S., Bell A., Duller G., Finch A., Jain M., King G., Pearce N., and Roberts M., Exploring Sources of Variation in Thermoluminescence Emissions and Anomalous Fading in Alkali Feldspars," *Radiation Measurements*, p. 06541, 2021.
- [10] David F., Walker F.D.L., Lee M. R., and Parsons I., Micropores and Micropermeable Texture in Alkali Feldspars: Geochemical and Geophysical Implications, *Mineralogical Magazine*, vol 59, pp. 505-534, 1995.
- [11] Whale T., Holden M., Kulak A., Kim Y., Meldrum F., Christ H., and Murray B., The Role of Phase Separation and Related Topography in The Exceptional Ice-Nucleating Ability of Alkali Feldspars, *Royal Society of Chemistry*, vol. 19, pp. 31186- 31193, 2017.
- [12] Hodson M., Micropore Surface Area Variation with Grain Size in Unweathered Alkali Feldspars: Implications for Surface Roughness and Dissolution Studies, *Geochimica et Cosmochimica Acta*, vol. 17, pp. 3429-3435, 2017. Huntley D., and Olav B., Some Observations on Tunnelling of Trapped Electrons in Feldspars and Their Implications for Dating, *Quaternary Science Reviews*, vol. 25, pp. 2503-2512, 2006.
- [13] Aitken M., *Thermoluminescence Dating*, *Quaternary Research*, vol. 26, pp. 280-281, 1986.
- [14] Weiyi J., Huabiao Y., Lizhu L., Huimin L., and Yen W., Phosphorescent Dynamics in SrAl<sub>2</sub>O<sub>4</sub>: Eu<sup>2+</sup>, Dy<sup>3+</sup> Single Crystal Fibers, *Journal of Luminescence*, vol. 76-77, pp. 424-428, 1998.
- [15] Gomez-Gonzalez M. A., Garcia-Guinea J., Garrido F., Townsend P., and Marco J., Thallium and Magnesium Complex Involved in The Luminescence Emission of Potassium-Bearing Aluminosilicates, *Journal of Luminescence*, pp. 197-206, 2015.
- [16] Finch A., and Klein J., The Causes and Petrological Significance of Chathodoluminescence emissions from Alkali Feldspars, *Contributions to Mineralogy and Petrology*, vol. 135, p. 234-243 , 1999.
- [17] Krbetschek K., Gütze J., Dietrich J.A., and Trautmann T., Spectral Information from Minerals Relevant for Luminescence Dating, *Radiation Measurements*, vol. 27, pp. 695-748, 1997.